Mariusz JAGIEŁA, Marcin KULIK

Opole University of Technology

doi:10.15199/48.2017.01.73

Cogging force and frequency bandwidth of a vibration energy harvester with nonlinear electromechanical resonance

Abstract. *The paper analyses the open-circuit frequency characteristics of a mechanical vibration energy harvester comprising of a single-coil cored armature and two vibrating yokes with permanent magnets connected to a plate spring. The cogging force, developed by action of the magnetic flux on the core brings a nonlinear component into system kinematics and causes complex variation of the frequency characteristics. It is shown that depending on dimensions of the generator parts, the system is capable of developing the frequency characteristics whose resonant frequency decreases or increases with the magnitude of external force. Through analysis supported by computer simulations using the finite element models it is shown that the systems with decreasing resonant frequency are more practical due to wider frequency bandwidth and higher amplitude of the generated voltage.*

Streszczenie. *W artykule analizowane są właściwości układu przetwarzania drgań mechanicznych w energię elektryczną zbudowanego z generatora liniowego z pojedynczą cewką z rdzeniem ferromagnetycznym oraz dwóch ruchomych jarzm z magnesami trwałymi połączonymi z metalową sprężyną paskową. Pokazano, że układ o takiej budowie może wytwarzać dwa rodzaje charakterystyk częstotliwościowych, tj. takie w których częstotliwość rezonansowa maleje lub rośnie wraz z amplitudą zewnętrznej siły wymuszającej drgania. Za pomocą symulacji komputerowych z wykorzystaniem modeli siatkowych, pokazano, że w układach praktycznych powinno dążyć się do osiągnięcia pierwszego typu charakterystyk ze względu na szersze pasmo częstotliwości oraz większą amplitudę generowanego napięcia.* ***Siła wewnętrzna i charakterystyki częstotliwościowe układu pozyskiwania energii z drgań mechanicznych z nieliniowym rezonansem elektromechanicznym***

Keywords: energy harvesting, mechanical vibrations, coupled problems.
Słowa kluczowe: pozyskiwanie energii elektrycznej z drgań mechanicznych, drgania mechaniczne, problemy sprzężone.

Introduction

Various types of electromechanical and electromagnetic converters are used as electrical energy generators in mechanical vibration energy harvesting systems [1-8]. Among them are those using, e.g. the piezoelectric or magnetostrictive effects [1, 2]. The electromechanical generators with permanent-magnet excitation are, however the most economically justified and basic structures [2-4]. In the most of cases the coreless generators are considered for this purpose [3-7]. The no-load (open armature circuit) frequency characteristic of such the harvester is identical with that of the second-order damped dynamical system. A minor impact of the nonlinearity, which originates of the mutual force due to action of the main flux on the armature current is visible only at loading condition. Such the force only slightly increases the resonant frequency, although the frequency bandwidth remains almost unaffected [3-5]. This is not the case in the recently proposed class of harvesters with the generators with cored armatures [6, 7]. The system of this type designed by authors of this is shown in Fig. 1.

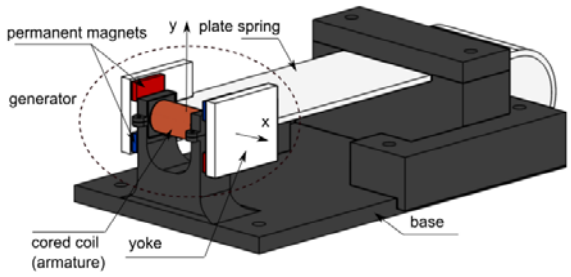

Fig.1. CAD drawing of considered mechanical vibration energy harvester.

Such the generator brings nonlinearity into kinematics of the entire system. The former is caused by the cogging force that comes from the action of the magnetic flux on the ferromagnetic core. It can be interpreted as an additional nonlinear spring connected in series with the linear one (plate spring connected to yokes).

By adjustment of the ratio taken between the linear spring factor and nonlinear one, the frequency bandwidth of the harvester can be significantly extended. However, due to complexity of the frequency characteristics development mechanism the design routine for such the system differs from that for one with the coreless generator. In order to provide correct operation within the desired frequency range the nonlinear oscillator theory should be involved in the designing. A simplified approach which can be used in design routine for such the system is presented in the following.

Basic theory

Assume that motion of yokes attached to spring in Fig. 1 is straight-line along the y-axis. In such the case the vectors of forces that act on the yoke have only the translational components. Assume also that the harvester operates at open-circuit conditions (no mutual force production). The balance of forces that act on for the moving yokes is

$$f_i + f_d + f_s = f_{ext} + f_{cog} \tag{1}$$

where: f_i, f_d, f_s are the inertia, damping and spring forces, while f_{ext} and f_{cog} are the external driving applied to the harvester base, and cogging forces, respectively. The dynamics of the system corresponding with (1) is described by the differential equation

$$m\ddot{y}_s + d\dot{y}_s + ky_s = f_{ext}(t) + f_{cog}(y_s) \tag{2}$$

where m, d, k, y_s are equivalent mass, damping constant, linear spring stiffness factor, and displacement of yokes, respectively. For further considerations it is convenient to express the cogging force through the spring factor k_{cog} as

$$f_{cog}(y_s) = k_{cog}(y_s)\,y_s \quad \text{with} \quad k_{cog}(y_s) = \frac{f_{cog}(y_s)}{y_s} \tag{3}$$

In this way the equation (2) can be considered in form

$$m\ddot{y} + d\dot{y} + \left(k - k_{cog}(y_s)\right)y_s = f_{ext}(t) \tag{4}$$

For considerations on the frequency characteristics the equation (4) will be linearized around y_s=0. Using the truncated Taylor series expansion and considering that $\lim_{y_s \to 0} k_{cog}(y_s) = \left(\partial f_{cog}/\partial y_s\right)_{y_s=0}$ one obtains

$$m\ddot{y}_s + d\dot{y}_s + (k - k_c)\, y_s = f_{ext}\ ;\ k_c = \left(\frac{\partial f_{cog}}{\partial y_s}\right)_{y_s=0} \tag{5}$$

Considering the quasi-dynamic condition, thus transforming (5) from time to frequency domain, one obtains the equation

$$-m\omega^2 \underline{Y}_s + i\omega d \underline{Y}_s + (k - k_c)\underline{Y}_s = \underline{F}_{ext} \tag{6}$$

with $i = \sqrt{-1}$, ω being the angular frequency and $y_s = \Im\mathrm{m}\left\{\underline{Y}_s e^{i\omega t}\right\}$, which has the two eigenvalues

$$\omega_{1,2} = \frac{id \pm \sqrt{4m(k - k_c) - d^2}}{2m} \tag{7}$$

Unlike the constants m and d that are real positive numbers, the spring factor k_c can be positive, negative or zero. The sign and value of k_c is dependent on internal configuration of the magnetic circuit. Considering only the eignevalue with positive real part the three cases can be distinguished.

a) No cogging force (coreless generator), thus k_c=0. Then system oscillates at its natural frequency identical with that of the second-order damped linear system defined by its mechanical configuration

$$\omega_n = \frac{id + \sqrt{4mk - d^2}}{2m} \tag{8}$$

b) The cogging force and the spring force have the same sense, thus $k_c < 0$. The fictitious linearized system operates at frequency increased with respect to natural frequency

$$\omega_u = \frac{id + \sqrt{4m(k + |k_c|) - d^2}}{2m} \tag{9}$$

c) The cogging force and the spring force have different senses, thus $k_c > 0$. The fictitious linearized system operates at frequency lowered with respect to natural frequency

$$\omega_l = \frac{id + \sqrt{4m(k - |k_c|) - d^2}}{2m} \tag{10}$$

From the above consideration it can be deduced that the three frequencies determine limits for the frequency bandwidth of a nonlinear system. Depending on the configuration of nonlinear system (sign of k_c) its frequency characteristics will be contained within the ranges of operation frequency ω_{op1} (ω_l, ω_n) if k_c>0 or ω_{op2} (ω_n, ω_u) if k_c<0. This simplified consideration should be augmented by the following notes.

- The sign of k_c is determined by internal configuration of the magnetic circuit. It is very sensitive to variation of dimensions of magnets and core. Each system has the operation frequency range ω_{op1} or ω_{op2} attributed to such the configuration. The natural frequencies of two systems having the operation ranges ω_{op1} and ω_{op2} can be different due to different masses m.

- The complexity of the frequency characteristics of the nonlinear system (2) goes far beyond the description given by the presented simple arithmetic which does not explain, e.g. the bistability phenomenon that the system exhibits at resonant frequencies. Moreover, it can be deduced from (4) that, depending on the configuration at certain points, the difference k-$k_{cog}(y_s)$ can be negative. The system will be unstable at these points not providing symmetry of motion. Work [6] has demonstrated that even when the difference is positive the system with k_c<0 can suffer from chaotic motion where the magnitude of vibrations is not proportional to the applied force. In continuation of this work we will demonstrate that the frequency characteristics of such the configuration are less practical due to smaller magnitude of the generated voltage and narrower frequency bandwidth.

Initially designed physical system

The specifications and dimensions of the magnetic circuit for the initially designed system are given in Tab. 1 and Fig. 2.

Table 1. Technical specifications of considered energy harvester

Property	Value
Spring length×width×height	100×50×3 mm
Spring material	Aluminium
Yoke length×c×d	40 ×6×35 mm
Yoke material	Mild steel
Magnet length×b×e	17×3×9 mm
Magnet material	NdFeB
Number of turns in the armature winding	100
Armature core material	Iron powder

The system has the linear spring constant k = 11800 N/m and the frequency characteristic with resonant frequency increasing with the magnitude of external force due to positive k_c equal to 1300 N/m. The natural frequency of the system is equal to 45.9 Hz, while the lower frequency limit to 43.6 Hz. The measured frequency characteristic of the rms value of open-circuit voltage is depicted in Fig. 3.

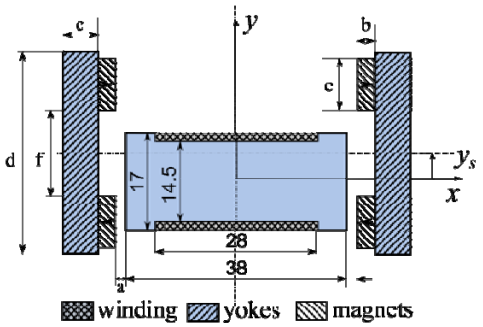

Fig.2. Cross-section of magnetic circuit with dimensions.

The characteristic was measured with the electromagnetic shaker fed with sinusoidal voltage, whilst the rms value of the current was kept constant as the frequency was increased from 35 to 50 Hz.

a)

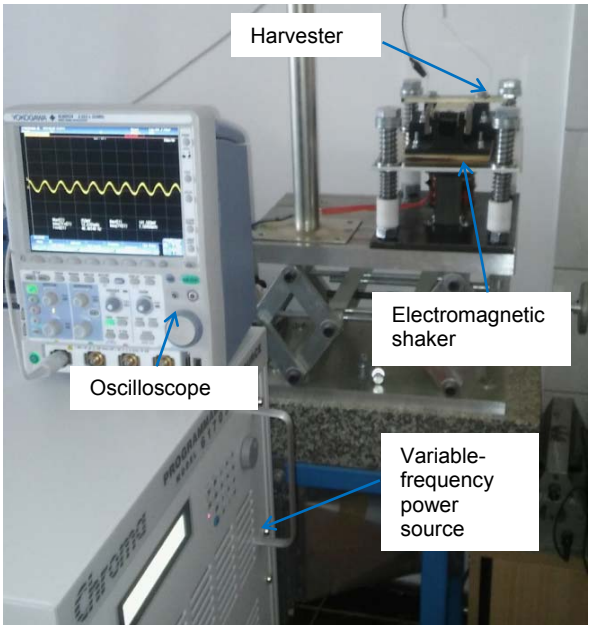

b)

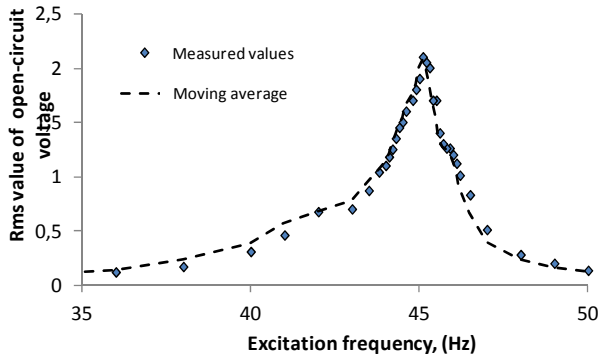

Fig.3. Frequency characteristic of open-circuit rms value of voltage: a) laboratory test-stand, b) results of measurements.

Even though the system has positive k_c, it does not suffer from chaotic motion, that could cause lack of proportionality between the excitation and operation frequencies. This is because the motion is determined by the spring force being one order of magnitude greater than the maximum value of the cogging force.

Models for determination of frequency characteristics

In computations the plate spring is considered as the distributed mechanical system. Determination of the frequency characteristics of the considered system is based on a solution of complex nonlinear equation of motion. The finite element equations derived from the Timoshenko cantilever-beam theory [8] read

$$(10)\quad -\omega^2\left(\boldsymbol{M}+\boldsymbol{M}_y\right)\underline{\boldsymbol{Y}}+i\omega\boldsymbol{D}\underline{\boldsymbol{Y}}+\left(\boldsymbol{K}-\boldsymbol{K}_{cog}\left(|\underline{\boldsymbol{Y}}|\right)\right)\underline{\boldsymbol{Y}}=\underline{\boldsymbol{F}}_{ext}$$

where $\boldsymbol{M}$ and $\boldsymbol{K}$ are distributed mass and stiffness matrices, whose derivation can be found in [8]. The matrix, $\boldsymbol{M}_y$ is the diagonal mass matrix attributed to the mass of yokes m_y such that $\boldsymbol{M}_y=0.5m_y\mathbf{diag}([1,1,1,1])$. The matrix $\boldsymbol{D}=\alpha\boldsymbol{M}+\beta\boldsymbol{K}$ is the damping matrix expressed by the Rayleigh model with the experimentally identified constants $\alpha=1.34\ 10^{-5}$ s, β=2.75 s^{-1}. The complex displacement vector $\underline{\boldsymbol{Y}}$ has the two translational components $\underline{Y}_1$ and $\underline{Y}_2$ along the y axis and the two rotating components $\underline{\Psi}_1$ and $\underline{\Psi}_2$ around the x axis $\underline{\boldsymbol{Y}}=[\underline{Y}_1,\underline{Y}_2,\underline{\Psi}_1,\underline{\Psi}_2]$ per single element [8]. The diagonal matrix $\boldsymbol{K}_{cog}(|\underline{\boldsymbol{Y}}|)$represents contribution of the cogging force to stiffness of the system in translational direction. It is calculated as $\boldsymbol{K}_{cog}=0.5\,k_{cog}^{eff}\,\mathbf{diag}([1,1,0,0])$ with k_{cog}^{eff} being the effective nonlinear spring factor due to the cogging force which is to be defined later on. The vector $\underline{\boldsymbol{F}}_{ext}=0,5\underline{F}_{ext}\,[1,1,0,0]^T$ represents the external force with the complex amplitude $\underline{F}_{ext}$ applied to the harvester base.

Determination of the cogging force is carried out via solution of the two-dimensional magnetostatic problem at different positions of yokes. The finite element equations governig the problem are considered in form

$$(11)\quad \boldsymbol{S}\left(B^2,y_s\right)\boldsymbol{\varphi}=\boldsymbol{\Theta}_{mag}$$

where $\boldsymbol{S}$ is the reluctance matrix dependent on the square of the magnetic flux density vector B^2 and position of yokes with respect to the armature, the vector of circulations of the magnetic vector potential, and $\boldsymbol{\Theta}_{mag}$ the vector of magnetomotive force due to permanent magnets [9]. Given the position of yokes y_s, the force $f_{cog}(y_s)$ is calculated from the Maxwell stress tensor [10].

The stiffness factor calculated using the instantaneous values of force and displacement using (3) cannot be used in the corresponding complex-valued problem (10). Transformation from the instantaneous-value-dependent to the amplitude-dependent stiffness factor is carried out demanding equality of the potential energy in both cases. The effective nonlinear stiffness factor dependent on the magnitude of sinusoidal vibration Y_s such that $y_s=Y_s\sin(u)$ is expressed as

$$(12)\quad k_{cog}^{eff}\left(Y_s\right)=\frac{2\int_0^{\pi/4} f_{cog}\left(Y_s\sin u\right)Y_s\cos u\,du}{Y_s^2}$$

Given operation frequency the no-load characteristics of the system are determined by iterative solution of (10) considering (12).

Computations

As is was outlined in the preceding sections, different frequency characteristics can be achieved in the considered system depending on the sign and value of k_c. In order to explore its potential to generate the frequency characteristics with high voltage and wide frequency bandwidth, we carried out the computer experiment in which we parametrized dimensions of some parts of the magnetic circuit, that are denoted by symbols in Fig. 3. Table 2 provides information about the parametrization. Each dimension was subdivided into 3 equal segments resulting in the grid covering the design space with 729 points.

Table. 3. Description of design variables

Description	Symbol in Fig. 2	Range of variation
Air-gap width	a	1.5-2.5 mm
Magnet thickness	b	3-4 mm
Yoke width	c	4-8 mm
Yoke height	d	20-40 mm
Magnet width	e	9-11 mm
Distance between magnets	f	15-18 mm

Normally in order to explore all 729 designs using the model (11) it would be necessary to determine complete variations of the cogging force and voltage induced in the winding, which would be too computationally extensive task.

We simplified the approach by restricting necessary computations to only two per single design by observation that in order to assess the potential performance of the system it is sufficient to know the factor k_c and the derivative of the magnetic flux linkage with respect to displacement y_s at $y_s=0$. These quantities are approximated by the finite differences

$$k_c \approx \frac{f_{cog}\left(\Delta y_s\right) - f_{cog}\left(-\Delta y_s\right)}{2\Delta y_s} \tag{13}$$

$$\left(\frac{\partial \lambda}{\partial y_s}\right)_{y_s=0} \approx \frac{\lambda\left(\Delta y_s\right) - \lambda\left(-\Delta y_s\right)}{2\Delta y_s} \tag{14}$$

where: Δy_s is a small displacement applied to the yoke, and is the magnetic flux inkage.

The computations were executed in a queue generating new finite element mesh according to the geometry specified for each design and performing computations of the two above defined quantities using model (11). As the computations were completed from the total number of 729 designs those with the highest absolute values of quantities (13) and (14) were selected. The above means that there are designs with positive and negative k_c. The results for the six most favored designs are compared in Fig. 4.

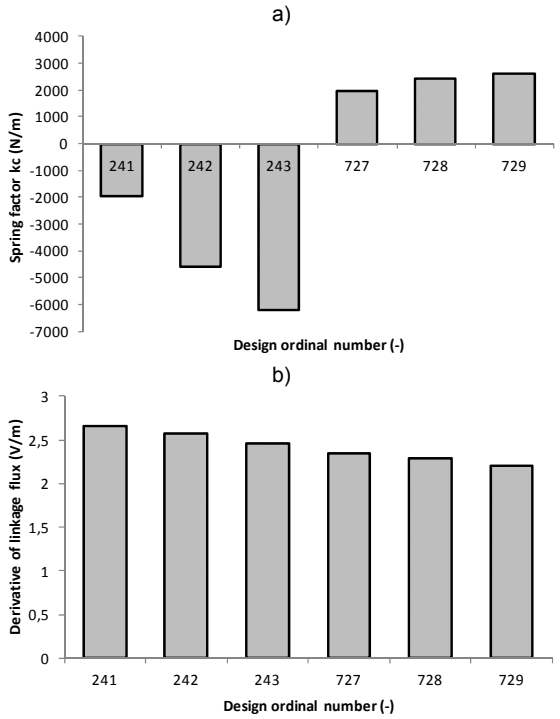

Fig. 4. Comparison of computed spring factors (13) and derivatives of magnetic flux linkage (14) for six selected designs.

The finally emerged designs are those with ordinal numbers 243 and 729 due to highest absolute values of k_c, thus potentially the widest frequency bandwidth. A surprising result is that the only different dimension for the two designs is the air-gap width being equal to 1.5 mm and 2.5 mm for the design 243 and 729, respectively.

The change of sense of the cogging force due to rise of the air-gap width is not the phenomenon that one would expect, although it is confirmed by change of the magnetic flux distribution in the air-gap regions in Fig. 5. Since the remaining dimensions are the same for the two designs, their masses are not affected and their the natural frequencies are the same.

In figure 6 the variations of cogging forces, effective spring factors k_{cog}^{eff} derivatives of the magnetic flux linkage are compared for both designs.

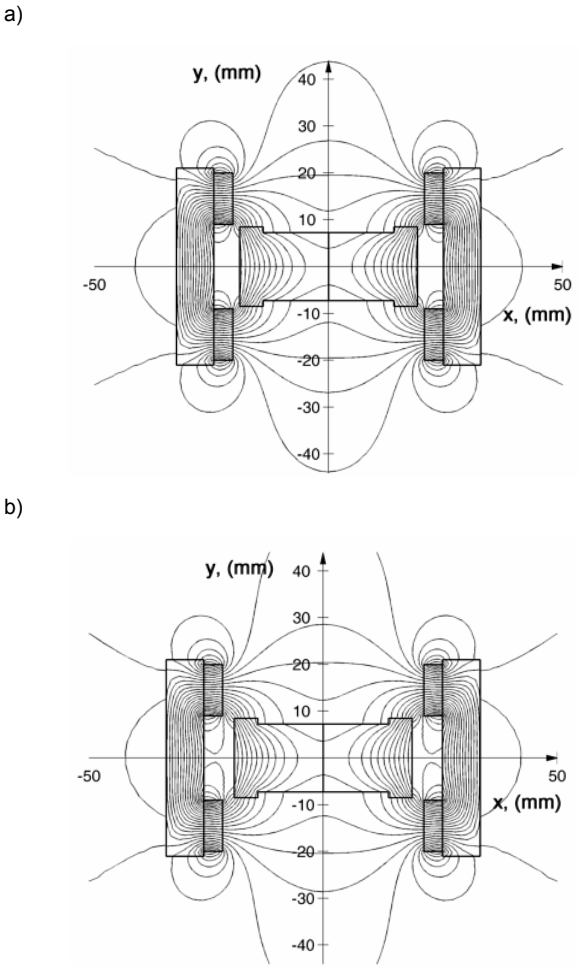

Fig. 5. Distributions of magnetic flux at y_s=0 for most favored designs: a) design 243 with positive k_c, b) design 729 with negative k_c.. Design 729 has wider air-gap.

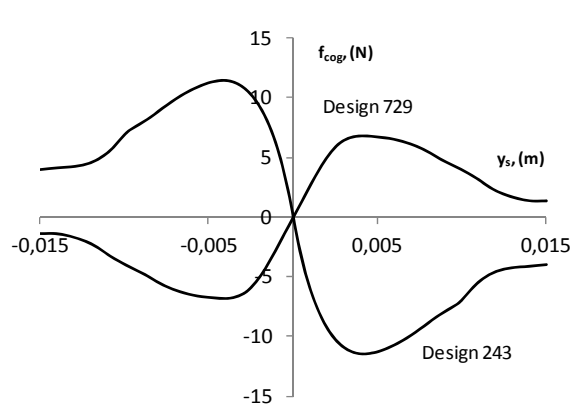

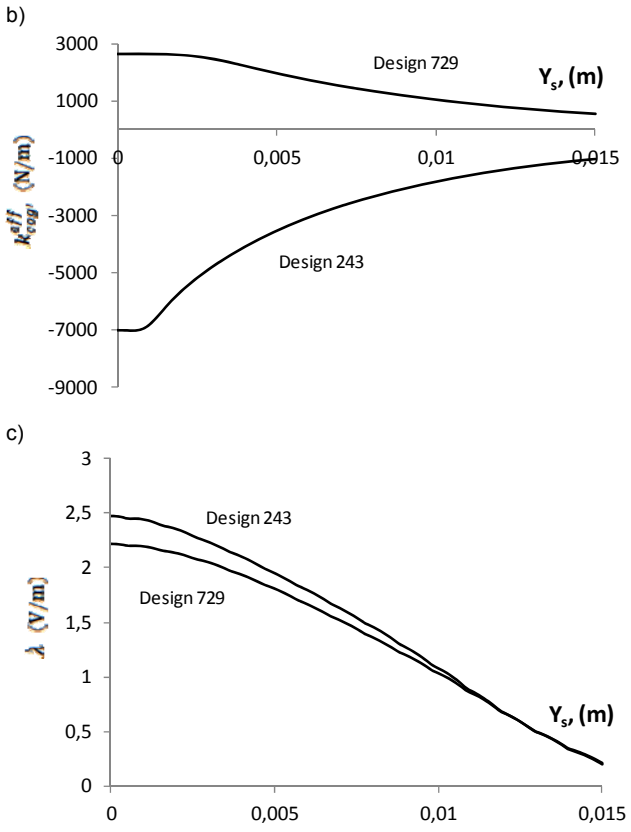

Fig. 6. Computed quantities: a) variations of effective spring factors, b) variations of derivatives of the magnetic flux linkage for the most favoured design 243 with positive k_c and design 729 with negative k_c.

Figure 7 depicts the frequency characteristics of rms value of generated open-circuit voltage.

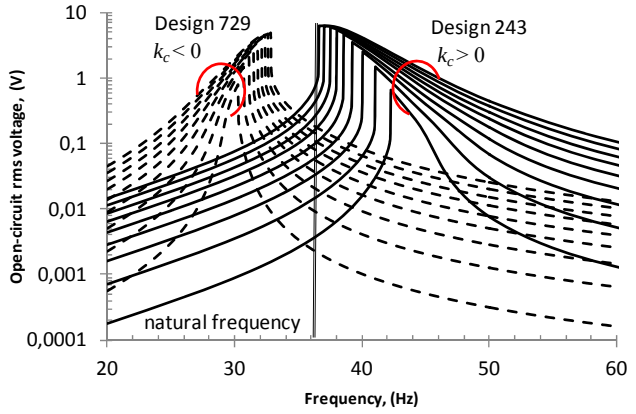

Fig. 7. Computed frequency characteristics of open-circuit voltage for design 243 (solid line) with positive k_c and design 729 (dashed line) with negative k_c for magnitude of external force ranging from 10 per cent to 90 per cent of maximum value of the cogging force.

The characteristics in Fig. 7 were obtained by solving equation (10) for nine magnitudes of the external force $|\underline{E}_{ext}|$ ranging from 10 to 90 per cent of maximum value of the cogging force. Each characteristic was obtained with the frequency sweep from 20 to 60 Hz. The rms value of the generated open-circuit voltage was obtained based on the computed complex magnitudes of displacement and the variations in Fig. 6c.

From the results of computations it becomes clear that the system with negative k_c provides much better performance than the one with positive k_c. The frequency bandwidth for the former is nearly two time as wide as for the latter, whilst the rms value of the generated open-circuit voltage is greater by some 30 per cent.

Conclusions

The type of frequency characteristics as well as the overall performance of the considered vibration energy harvester are strongly dependent on design of the generator magnetic circuit. The performance of the initially designed physical system do not exploit full potential of the considered structure. The presented methodology was used in designing new harvester which is currently under construction.

***Authors**: dr hab. inż. Mariusz Jagieła, Prof. PO, mgr inż. Marcin Kulik, Politechnika Opolska, Instytut Układów Elektromechanicznych i Elektroniki Przemysłowej, ul. Prószkowska 76, 45-758 Opole, E-mail: m.jagiela@po.opole.pl, marcin.kulik@doktorant.po.edu.pl.*

REFERENCES

[1] Challa V. R., Prasad M. G., Shi Y., Fisher F. T., A vibration energy harvesting device with bidirectional resonance frequency tunability, *Smart Materials and Structures*, 17 (2008), No. 1, IOP Science Publ., 1-11.

[2] Chen S.M., Zhou J.J., Hu J.H., Experimental study and finite element analysis for piezoelectric impact energy harvesting using a bent metal beam, *Int. Journ. of Applied Electromagnetics and Mechanics*, 46 (2014), No. 4, IOS Press, 895-904.

[3] Williams C.B., Shearwood C., Harradine M.A., Mellor P.H., Development of an electromagnetic microgenerator, *IEE Proc. Circuits, Devices and Systems*, 148 (2001), No. 6, 337-342.

[4] Beeby S. P., Torah R. N., Tudor M. J., Glynne-Jones P., O'Donnell T., Saha C. R., Roy S., A micro electromagnetic generator for vibration energy harvesting, *Journal of Micromechanics and Microengineering*, 17(2007), IOP Publishing, 1257-1265.

[5] Gieras J.F., Oh J.H., Huzmezan M., Electromechanical energy harvesting system, *Int. Patent Publ.* WO 2007/044008 A1, 2011.

[6] Sato T., Igarashi H., A new wideband electromagnetic vibration energy harvester with chaotic oscillation, *Journal of Physics, Conf. Series, 476 (2013), Conference 1*, IOP Science Publ. 2013, Article No. 012119.

[7] Sato T., Watanabe K., Igarashi H., Coupled analysis of electromagnetic vibration energy harvester with nonlinear oscillation, *IEEE Trans. Magn.*, 50 (2014), No. 2, Article No. 7007604.

[8] Ferreira A.J.M., Matlab codes for finite element analysis, Solid mechanics and its applications 157, Springer, Netherlands, 2009.

[9] Demenko A., Sykulski J.K., Network equivalents of nodal and edge elements in electromagnetics, *IEEE Trans. Magn.*, 38 (2002), No. 2, 1305-1308.

[10] Demenko A., Mendrela E.A., Szelag W., Finite element analysis of saturation effects in tubular linear generator, *The Intern. Journ. for Comp. and Math. in Electrical and Electronic Eng. COMPEL*, 25 (2006), No. 1, 43-54.